UMT PRESS

Journal of Mathematical Sciences and Informatics
Journal Homepage: https://journal.umt.edu.my/index.php/jmsi
eISSN: 2948-3697
DOI: http://doi.org/10.46754/jmsi.2025.12.004

THIN FILM BOUNDARY LAYER FLOW OF WATER-BASED HYBRID NANOFLUIDS ALONG WITH AN APPLIED MAGNETIC FIELD: AN ANALYTICAL APPROACH

ALI REHMAN[1]*, ZABIDIN SALLEH[1] AND K. SUDARMOZHI[2]

[1]Faculty of Computer Science and Mathematics, Universiti Malaysia Terengganu, 21030 Kuala Nerus, Terengganu, Malaysia. [2]Department of Mathematics, Saveetha School of Engineering, Saveetha Institute of Medical and Technical Sciences, Chennai, Tamil Nadu, India.

**Corresponding author: alirehmanchd8@gmail.com*

ARTICLE INFO

Article History:
Received 3 August 2025
Revised 6 October 2025
Accepted 10 October 2025
Published 15 December 2025

Keywords:
Water-based hybrid nanofluid;
Homotopy Asymptotic Method;
magnetohydrodynamics;
stretching surface.

ABSTRACT

This research presents an analytical examination of the steady-state boundary layer flow and thermal characteristics of hybrid nanofluid systems. Both nanofluid and hybrid formulations are analysed; a similarity transformation recasts governing partial differential equations into ordinary differential forms. The derived system is tackled using the Homotopy Asymptotic Method (HAM), which provides closed-form analytical solutions that contribute to an understanding of the flow behaviour. The researcher produces visual representations of the flow and temperature fields for the different cases and performs a convergence analysis using the BVPh 2.0 software, which involves 25 iterative cycles. The skin friction coefficient and Nusselt number are two key parameters. The results serve as a fundamental step for engineering applications of advanced fluid mechanics, which include the manufacture of materials, the transport of biomedicals, cooling systems, and thermal management.

2020 Mathematics Subject Classification: 65M25, 76W05

Introduction

Recently, there has been a growing focus on hybrid nanofluids, an advanced category of nanofluids, as researchers continue to explore this field. Hybrid nanofluids can be designed in two fundamental ways: (i) Using two or multiple different nanoparticles and dispersing them in a base fluid, or (ii) Using composite nanoparticles and incorporating them in a fluid. It is the hybrid nanofluids' ability to enhance the heat transfer properties of conventional nanofluids that makes them a promising area of research. However, the literature on hybrid nanofluids is still relatively sparse. Suresh *et al*. [1] found that hybrid nanofluids attain higher Nusselt numbers than regular nanofluids and improve laminar convective heat transfer. In a later work, Suresh *et al*. [2] stated that the hybrid nanofluid energy transfer rate was 8.02% greater than that of a single-nanoparticle fluid. Selvakumar *et al*. [3] experimentally demonstrated that a hybrid nanofluid as a coolant in heat sinks enhances the convective heat transfer coefficient. Needing no authentication, Nasrin *et al*. [4] research on forced convection in a horizontal plate solar collector is centred on cooled hybrid (alumina–copper) and heated single (alumina) nanofluids and determined that the cooled hybrid delivered enhanced thermal performance.

The boundary layer equations, their derivation, and solution through similarity transformations, remain a primary focus within the field of fluid mechanics. For Newtonian and non-Newtonian fluids, the boundary layer theory serves as a significant analytical modelling construction, and the

theoretical predictions of boundary layer modelling tend to be consistent with the outcomes of most experimental observations. Non-Newtonian fluids are utilised in various industries, including engineering with polymers, food processing, petroleum drilling, and the paper-making process. The development of governing models for non-Newtonian fluids has proven to be challenging, as they often exhibit non-linear stress-strain relations. Notwithstanding, there are processes such as food processing, polymer extrusion, metal spinning, fibre coating, and hot rolling, where non-Newtonian fluids, especially boundary layer flows, play a crucial role.

In recent years, there has been a growing focus on the Sisko fluid model. Due to its engineering relevance, Sisko fluids have been investigated in a varied range of studies, including, studies by Munir *et al*. [5] on bidirectional flows over an extending sheet, Olanrewaju *et al*. [6] on unsteady free convection past a flat plate, Khan *et al*. [7, 8] on annular pipe and stretching surface flows, Patel *et al*. [9] on the Sisko laminar boundary layer, Darji *et al*. [10] on unsteady natural convection, and Siddiqui *et al*. [11] on film flows over vertical belts. Malik *et al*. [12] and Nadeem *et al*. [13] made significant contributions to the study of Eyring–Powell nanofluid flow with Magnetohydrodynamic (MHD) and mixed convection, as well as the study of Maxwell fluid over a surface with nanoparticles, respectively. Raju *et al*. [14] reported on MHD nano-non-Newtonian fluid flow over a cone integrated with energy and mass transfer, while Rokni *et al*. [15] presented a study about nanoparticle suspension between plates. Following that, Jeffery nanofluid MHD flow [16, 17], Al_2O_3–water nanofluids [18], the use of Al_2O_3 as a coolant in diesel generators [19], and turbulent flow of Al_2O_3–$C_2H_6O_2$ and CuO–$C_2H_6O_2$ suspensions [20] were studied.

The study of non-conventional shapes and conditions has also been done. Sebdani *et al*. [21] researched tetragonal cavities, while Gul *et al*. [22, 24] focused on the shape of particles and studied ferrofluids and magnetic fields. Ahmed *et al*. [23] investigated the effects of geometry on particles. The study of Marangoni convection in CNT-based nanofluids was investigated by Rehman *et al*. [25, 34], as well as the effect of viscous dissipation in thin films [26]. The theoretical and practical importance of nanofluids and hybrid nanofluids is undeniable. In particular, hybrid formulations almost always show an improvement in heat transfer performance, demonstrating their greater potential in various industrial, engineering, and scientific fields. The Homotopy Asymptotic Method (HAM) is used to obtain the analytical solution, having been first applied to non-linear problems by Liao *et al*. [27]. The method is known for its rapid convergence to near solutions.

The series solution is constructed as a functional form that encapsulates all the theoretical parameters. The effect of these parameters is analysed in detail and systematically in the magnetic field, which has been isolated and discussed, as well as in hybrid nanofluid stagnation point flows [35]. Other notable contributions include the application of Keller-box techniques to MHD bio-viscosity flow [29], the analysis of a thermal boundary layer with non-linear radiation [30], and the investigation of couple-stress nanofluids with varying viscosities [32, 33]. Khan *et al*. [40-41] studied the unsteady flow of nanofluid over a vertical plate and a permeable surface. Rehman *et al*. [42] study Marangoni convection in stagnation point flow of a blood-based carbon nanotube nanofluid across an unstable stretching surface is being studied scientifically. Khan *et al*. [43-44] studied a comparative case study of entropy generation in MHD conjugate flow. Nisar *et al*. [45] studied heat transfer and entropy creation when drilling clay nanoparticles into nanoliquids.

Mathematical Formulation

Consider the steady flow of a hybrid nanofluid and base fluid via a stretching surface in the presence of a magnetic field. $M = \frac{\sigma B_0^2}{\rho}$ and stretching parameter $A = \frac{b}{c}$. In this combination, Cu + Water represents the base fluid and $\mathrm{Cu} + Al_2$ + Water represents a hybrid nanofluid. The continuity and momentum equations are given below. All other assumptions are selected as [28]:

$$\frac{\partial u}{\partial x} + \frac{\partial v}{\partial y} = 0, \tag{1}$$

$$u\frac{\partial u}{\partial x} + v\frac{\partial v}{\partial y} = \varepsilon\frac{\partial^2 u}{\partial y^2} - \frac{\sigma B_0^2}{\rho}u, \tag{2}$$

$$u\frac{\partial T}{\partial x} + v\frac{\partial T}{\partial y} = \alpha\frac{\partial^2 T}{\partial y^2} + \frac{K}{c_p}\left(\frac{\partial u}{\partial y}\right)^2. \tag{3}$$

Here, u and v denote the velocity component along x and y direction, the kinematic viscosity of the fluid is represented by $\nu = \frac{\mu}{\rho}$. The temperature of the fluid is meant by T, the thermal diffusivity of the fluid is denoted by $\alpha = \frac{k}{\rho c}$, where k shows the thermal conductivity and ρc is the fluid capacity, heat, and c_p is specific heat. The corresponding boundary condition is given by:

$$u = 0, T = T_w(x) \text{ at } y = 0, \tag{4}$$

$$u = U, T = T_\infty \text{ at } y \to \infty. \tag{5}$$

Thermophysical properties of hybrid nanofluid:

$$\rho_{hnf} = \phi_2\rho_{AlO_2} + \left[\left(1-\phi_1\right)\rho_f + \phi_1\rho_{Cu}\right]\left(1-\phi_2\right),$$

$$\mu_{hnf} = \mu_f\left(1-\phi_1\right)^{-2.5}\left(1-\phi_2\right)^{-2.5},$$

$$\left(\rho c_p\right)_{hnf} = \phi_2\left(\rho c_p\right)_{AlO_2} + \left[\left(1-\phi_1\right)\left(\rho c_p\right)_f + \phi_1\left(\rho c_p\right)_{Cu}\right]\left(1-\phi_2\right),$$

$$k_{hnf} = \frac{k_{AlO_2} + 2k_{nf} - 2\phi_2\left(k_{nf} - k_{AlO_2}\right)}{k_{AlO_2} + 2k_{nf} + \phi_2\left(k_{nf} - k_{AlO_2}\right)} \times \frac{k_{Cu} + 2k_{nf} - 2\phi_1\left(k_{nf} - k_{Cu}\right)}{k_{Cu} + 2k_{nf} + \phi_1\left(k_{nf} - k_{Cu}\right)}.$$

The dimensionless variable is defined as:

$$\eta = y\sqrt{\frac{U}{\nu x}}, \psi = \sqrt{U\nu f(\eta)}, u = \frac{\partial\psi}{\partial y} = Uf'(\eta),$$

$$v = -\frac{\partial\psi}{\partial x} = \frac{1}{2}\sqrt{\frac{U\nu}{x}}\left(\eta f' - f\right), \theta(\eta) = \frac{T - T_\infty}{T_w - T_\infty}. \tag{6}$$

Equation (6) fulfilled Equation (1) and reduced Equations (2) and (3) in the following form:

$$\frac{1}{\left(1-\phi_1\right)^{2.5}\left(1-\phi_2\right)^{2.5}\left[\left\{\left(1-\phi_2\right)\left(1-\phi_1+\phi_1\frac{\left(\rho\right)_{Cu}}{\left(\rho\right)_f}\right)\right\}+\phi_2\frac{\left(\rho\right)_{AlO_2}}{\left(\rho\right)_f}\right]}f'''+ff''-\frac{\sigma_{hnf}\rho_f}{\sigma_f\rho_{hnf}}Mf'=0, \tag{7}$$

$$\frac{1}{\left(1-\phi_1\right)^{2.5}\left(1-\phi_2\right)^{2.5}\left[\left\{\left(1-\phi_2\right)\left(1-\phi_1+\phi_1\frac{\left(\rho C_p\right)_{Cu}}{\left(\rho C_p\right)_f}\right)\right\}+\phi_2\frac{\left(\rho C_p\right)_{AlO_2}}{\left(\rho C_p\right)_f}\right]}\theta''+\frac{1}{2}\theta'+$$

$$\Pr Ec\frac{\mu_{hnf}\rho_f}{\mu_f\rho_{hnf}}\left(f''\right)^2-\eta pr\left(f'\theta\right)=0, \tag{8}$$

with boundary condition:

$$f'=0, f=0, \theta=1 \text{ at } \eta=0, \tag{9}$$

$$f'(\infty)=1, \theta(\infty)=0. \tag{10}$$

The skin friction coefficient C_{nf} is well-defined as $C_{nf}=\frac{\tau_w}{\frac{1}{2}\rho U_w^2}$ and the local Nusselt number $Nu_x = Nu=\frac{q_w}{k(T_w-T_0)}x$.

Method of Solution

The mentioned Equations (7) and (8) are resolved analytically using the Homotopy Asymptotic Method (HAM), as shown below:

$$L\left(u\left(x\right)\right)+N\left(u\left(x\right)\right)+g\left(x\right)=0, B\left(u\left(x\right)\right). \tag{11}$$

In this formulation, L represents the linear operator, x is the independent variable, $g(x)$ is the unknown function, N is the non-linear operator, and $B(u)$ is the boundary operator. As the first step in this method, one constructs a family of equations that continuously vary from a given approximation to the complete solution of the original problem.

$$H\left(\phi\left(x\right),p\right)=\left(1-p\right)\left[L\left(\phi\left(x,p\right)\right)+g\left(x\right)\right]-H\left(p\right)\left[L\left(\phi\left(x,p\right)\right)+g\left(x\right)+N\left(\phi\left(x,p\right)\right)\right]=0$$
$$B\left(\phi\left(x,p\right)\right)=0. \tag{12}$$

Here, p is the embedding parameter which varies within the interval [0,1]. The function $H(p)$ is a nonzero auxiliary function for p ≠ 0 satisfying $H(0)=0$. Moreover, ϕ(x,p) is the unknown function that needs to be found. Using the first guessed values with auxiliary linear operators defined in Equations (7) and (8). The homotopy equation is formed. This equation smoothly changes the initial approximation into the exact solution when (p) moves from 0 to 1.

$$f_0(\eta) = \frac{c}{a}\eta, \tag{13}$$

$$L_f = \frac{d^3 f}{d\eta^3}, \quad L_\theta = \frac{d^2\theta}{d\eta^2}, \tag{14}$$

with constant properties

$$L_f\left(C_1 + C_2\eta + C_3\eta^2 + C_4\eta^3\right) = 0 \quad \text{and} \quad L_\theta\left(C_5 + C_6\eta\right) = 0. \tag{15}$$

The constants [C_i (i = 1, 2, \dots, 6)] are constants on the general solution. To assess the quality of the approximation, we used the average squared residual error introduced by Liao [36]. Accordingly, Equations (7) and (8) may be restructured to focus on minimising the residual error, closing the series solution. This enables the determination of the optimal solution. Hence, the solution becomes more dependable and precise.

$$\varepsilon_m^f = \frac{1}{n+1}\sum_{j=1}^{n}\left[\kappa_f\left(\sum_{j=1}^{n} f(\eta)_{\eta=j\delta\eta}\right)\right], \tag{14}$$

$$\varepsilon_m^\theta = \frac{1}{n+1}\sum_{j=1}^{n}\left[\kappa_\theta\left(\sum_{j=1}^{n} f(\eta)_{\eta=j\delta\eta}, \sum_{j=1}^{n}\theta(\eta)_{\eta=j\delta\eta}\right)\right]. \tag{15}$$

Results and Discussions

Table 1: Assessment of the skin friction for the 2 nanofluids when $Pr = 11.6, \phi = 0.5, A = 0.7$

$\boldsymbol{\beta}$	$\boldsymbol{M}$	$\boldsymbol{Cu + Water}$	$\boldsymbol{Cu + Al_2 + Water}$
0.3	7	0.229705	0.19471
0.5		0.22164	0.179547
0.7		0.21147	0.17264
	8	0.2100877	0.16994
	9	0.17608	0.13724
		0.168432	0.1246
		0.15818	0.11641

Table 2: Evaluation of the Nusselt number $(Re_x^{-\frac{1}{2}} Nu_x)$ for the 2 nanofluids when $\beta = 0.9, M = 5, A = 0.9$

$\boldsymbol{Pr}$	$\boldsymbol{Ec}$	$\boldsymbol{Cu + Water}$	$\boldsymbol{Cu + Al_2 + Water}$
10	3	0.91231	0.99077
15		0.89341	0.88237
20		0.67451	0.87397
	5	0.35614	0.75647
	7	0.23776	0.74897
		0.22795	0.63121
		0.15021	0.61346

Table 3: Shows the convergence of the system for $Cu + Al_2 + Water$ while $Pr = 6, M = 10, Ec = 1, \nu = 1, A = 1$

m	$\varepsilon_m^f Cu + Al_2 + Water$	$\varepsilon_m^\theta Cu + Al_2 + Water$
5	5.36438×10^{-1}	2.86775×10^{-1}
10	7.14094×10^{-3}	1.48738×10^{-2}
15	3.209443×10^{-7}	1.07298×10^{-4}
20	4.37298×10^{-9}	8.54131×10^{-5}
25	1.95787×10^{-11}	7.94423×10^{-6}

Table 4: Shows the convergence of the technique for $Cu + Water$ during $Pr = 8, M = 5, Ec = 5, \beta = 0.1, A = 0.9$

m	$\varepsilon_m^f Cu + Water$	$\varepsilon_m^\theta Cu + Water$
5	1.07991×10^{-1}	2.88574×10^{-1}
10	5.65266×10^{-2}	1.0759×10^{-3}
15	4.12383×10^{-3}	1.0759×10^{-5}
20	3.4616×10^{-4}	8.55721×10^{-7}
25	3.133×10^{-5}	8.006632×10^{-9}

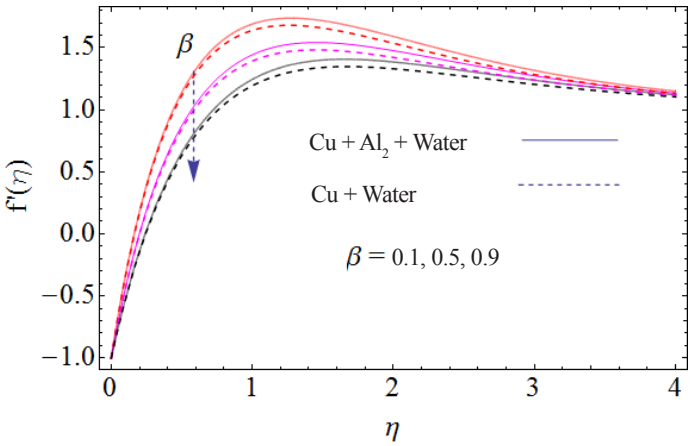

Figure 1: Effect of thin film thickness parameter on $f'(\eta)$

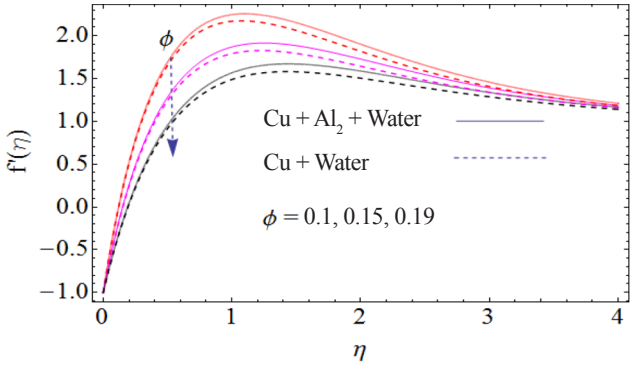

Figure 2: Result of dimensionless nanoparticle volume fraction on $f'(\eta)$

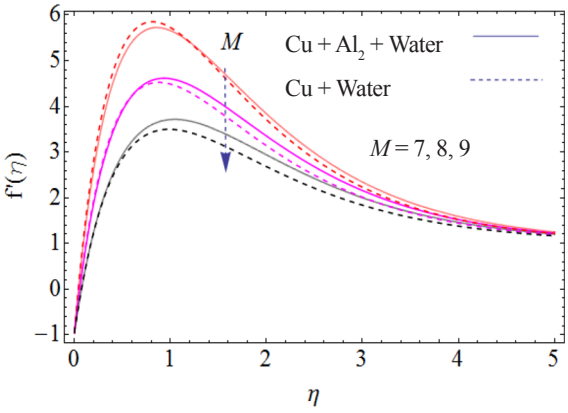

Figure 3: Result of magnetic field M on $f'(\eta)$

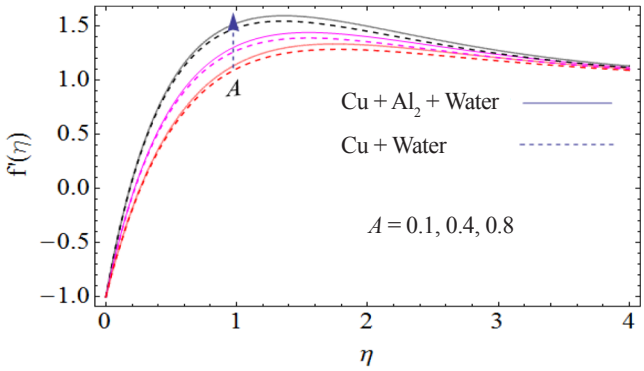

Figure 4: Result of stretching parameter A on $f'(\eta)$

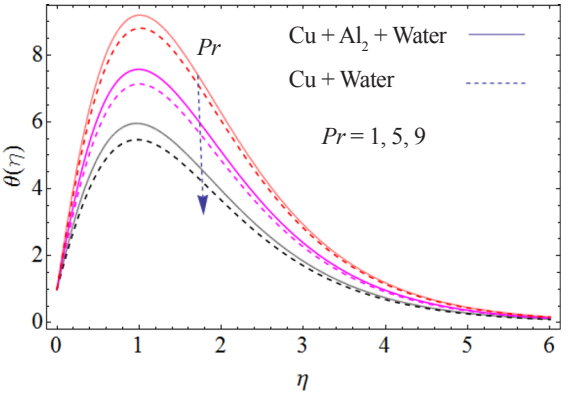

Figure 5: Result of Pr versus $\theta(\eta)$

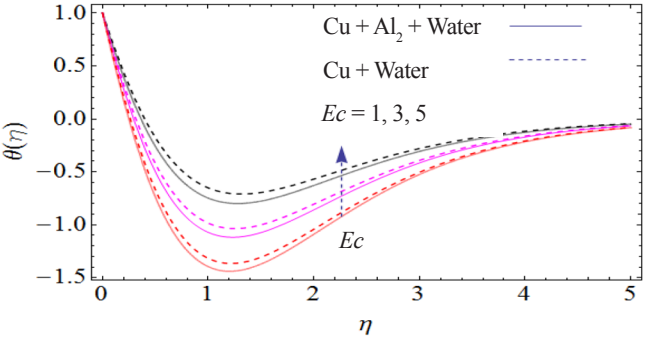

Figure 6: Effect of Ec on the $\theta(\eta)$

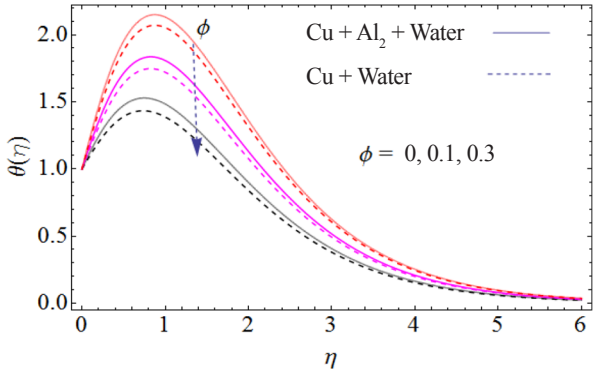

Figure 7: Result of dimensionless nanoparticle volume fraction on $\theta(\eta)$

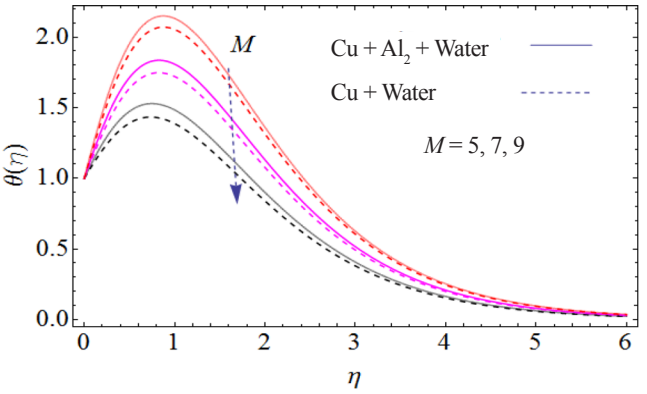

Figure 8: Result of the magnetic field on the temperature profile

In this analysis, Cu + Water is treated as the base nanofluid and Cu + Al_2O_3 + Water is treated as the hybrid nanofluid. The focus is primarily to evaluate the impact of multiple model parameters, thin film thickness parameter β, M, stretching parameter (A), Prandtl number (Pr), Ec, and ϕ on the distribution of the velocity and temperature. These include numerical results presented in Tables 1 to 4 and the Figures 1 to 8. Illustrations are included to enhance the understanding of the findings further.

Tabulated Results: Skin Friction and *Nu*

In the context of the results included in the report, Tables 1 and 2 contain the variation of the cf and the Nusselt number for both Cu + Water and Cu + Al_2O_3 + Water nanofluids. The skin friction coefficient is observed to decrease with an increase in β and M, indicating a reduction in skin friction as the magnetic field and film thickness increase. This is because, in the limit of a neglected magnetic field, a larger resistance layer is produced, thereby reducing the fluid's freedom to move near the surface.

Table 2 provides evidence that higher values of the Prandtl and Eckert numbers correlate with a decrease in the Nusselt number. A surge in Pr decreases the thermal boundary layer thickness. Consequently, heat transfer to the fluid decreases, which results in a lower Nusselt number. This occurs because fluids with higher Prandtl numbers (especially oils) have a dominant thermal momentum diffusion. In the case of Ec, a rise in the Eckert number represents more substantial viscous dissipation, meaning a fraction of the mechanical work is converted into internal heat. This self-heating effect reduces the temperature gradient at the wall, resulting in a lower Nusselt number.

The iterative convergence of both nanofluids is illustrated in Tables 3 and 4. In both systems, convergence is achieved within 25 iterations, accompanied by a significant decrease in residual error with each iterative step. This highlights the stability and robustness of the numerical scheme employed.

Graphical Results: Velocity and Temperature Distributions

Influence of Thin Film Thickness Parameter (β) on Velocity (Figure 1)

The velocity profile $f'(\eta)$ becomes less pronounced (i.e., velocity decreases) when becomes larger. From a physical standpoint, when a film of greater thickness is present, film fluid particles experience greater drag from surface viscous interactions, hence, viscous forces become larger. This, in turn, causes fluid motion to become retarded, and velocity to decrease. This scenario is more exaggerated and pronounced in hybrid nanofluids. The reason is that a greater number of nanoparticles leads to high viscosity and inter-particle interactions, which further retards the motion of the hybrid nanofluid.

Influence of ϕ on Velocity (Figure 2)

The velocity profile is improved (i.e., becomes less pronounced) when ϕ is greater. The reason is that the addition of more nanofluids results in a rise in both the viscosity and density of the fluid. The increase in interparticle interactions must also be taken into account. The hybrid nanofluid containing both Cu and Al_2O_3 particles, shows greater velocity deficits as compared to the simple Cu-water system (because of the increased solid fraction and more pronounced particle-fluid interactions). The reason is that, although thermal conductivity (a mode of energy transfer) is improved, the flow of fluid is further restricted in the system. This is due to the large particle loads.

Effect of M on Velocity (Figure 3)

As increases, velocity still declines. This is due to an increase in the induced Lorentz force by the magnetic fields and a rise in the conversion of the fluid's kinetic energy to Joule heat. This magnetic fluid friction slows the movement of the $f'(\eta)$ and the decline in velocity. The hybrid nanofluids exhibit stronger suppression due to their higher electrical conductivity.

Effect of A on Velocity (Figure 4)

The increase in A corresponds to a rise in the $f'(\eta)$. A surge in the stretching parameter intensifies the stretching of the surface, allowing fluid layers to be dragged more easily. This, in turn, increases fluid momentum and further enhances the velocity profile. The increase in velocity is more than that of the base nanofluids due to the increase in thermal conductivity of the hybrid nanofluids.

Effect of Pr on Temperature (Figure 5)

The increase in Pr corresponds to a decline in the temperature outline. The growth of the Prandtl number also indicates a reduction in thermal diffusivity. In high fluids, momentum is diffused more, resulting in a thinner thermal boundary layer and increased heating of the liquid. The fluid loses heat, resulting in a decline in the temperature contour. Hybrid nanofluids enhance the effect by accelerating heat dissipation.

Impact of Ec on Temperature (Figure 6)

With growing Ec values, the temperature distribution profile improves. Bigger Eckert numbers imply the conversion of kinetic energy into internal energy through viscous dissipation, thus the local heating effect raises the temperature field in the boundary layer. This effect is more substantial for the hybrid nanofluid, which is due to the suspended nanoparticles increasing the particle–fluid interaction. Thus, the concentration of localised heating under viscous stress.

Impact of ϕ on Temperature (Figure 7)

As particle concentration increases, the temperature profile becomes more uniform. This is due to the solid fraction, which leads to more heat conduction being removed from the fluid, thereby decreasing the bulk temperature distribution, despite an increase in thermal conductivity. The added hybrid nanofluid remains more pronounced due to the heat conduction pathways that synergistically result from the Cu and Al_2O_3 nanoparticles.

Impact of M on Temperature (Figure 8)

As *M* increases, the temperature outline drops. The temperature reduction is due to the magnetic field being applied, which weakens motion through the Lorentz force, thus reducing convective currents and increasing energy dissipation. This effect is more pronounced in hybrid nanofluids due to greater electrical conductivity, which increases the Lorentz force, thus reducing it further.

Insights on Physical Behaviour

When assessing parameter variation, hybrid nanofluids ($Cu + Al_2O_3 +$ Water) demonstrated a higher degree of variability compared to the base nanofluid (Cu + Water), which can be explained by:

- The increased viscosity influenced the velocity distributions due to the suspension of multiple nanoparticles.
- The notable rise in thermal conductivity means the heat transfer is enhanced, although the temperature fields are reduced when thermal diffusion predominates.
- The greater electrical conductivity strengthens the Lorentz force under magnetic fields.
- The increased interaction of the particles with the fluid dissipative viscous forces and viscous heating become more pronounced.
- The combination of the above features depicts the dominant thermal-hydrodynamic performance of hybrid nanofluids and offers potential for deployment in more sophisticated thin film flows, thermally stressed, magnetic field applications, and high industrial engineering tasks.

Conclusions

The current study examines analytical solutions for steady boundary layer flow and heat transfer for both nanofluids and hybrid nanofluids. The application of a similarity transformation allows for the governing Partial Differential Equations (PDEs) to be simplified into Ordinary Differential Equations (ODEs). The Optimal Optimal Homotopy Asymptotic Method (OHAM) is utilised to solve the resulting non-linear problem. This method is specially designed to provide analytical approximations for strongly non-linear systems. This method offers an opportunity to understand the velocity and temperature distributions for different governing parameters. The results are obtainable graphically for the velocity and temperature fields, and the skin friction coefficient and Nusselt number are tabulated for easier access and interpretation. The analytical series solutions were proven to be convergent within the BVPh 2.0 package for a computational order of 25, indicating reliability. Hybrid nanofluids are the focus of the current study, aiming to confirm their superiority in terms of thermal conductivity, viscosity, and particle–fluid interactions. These are amplified for every tested case of the current study. The effect of the boundary layer is confirmed for the system, as the temperature and velocity profiles were observed to move in parallel, providing relative proof of axial support.

Findings of this research are:

- Impact of thin film thickness (β): An increase in equates to a reduction in the velocity profile. This can be explained as a consequence of additional film thickness creating more viscous resistance in the boundary layer. Therefore, the fluid particles are more restrained, resulting in a decrease in velocity.
- Impact of stretching parameter (A): A rise in A improves the velocity outline. This acceleration of the boundary layer flow is due to effective stretching that can drag adjacent fluid layers, thereby enhancing the momentum of particles.
- Impact of Prandtl number (Pr): The rise in Pr results in a decline in the temperature profile. The fluid with a high Pr has weaker thermal diffusion relative to momentum diffusion, thus resulting in thinner thermal boundary layers and a lesser quantity of heat transferred into the fluid.
- Impact of Eckert number (Ec): A rise in Ec results in a more elevated temperature profile. Larger values of Ec are associated with stronger viscous dissipation processes where conversion of kinetic energy into thermal energy occurs, thus raising the temperature of the fluid.
- Impact of magnetic field (M): A surge in M results in a decline in velocity. The Lorentz forces created by the applied magnetic field counteract the fluid motion, thereby creating an additional resistance due to the charged particles within the fluid, which results in damping of the velocity contour.
- The impact of varying the ϕ of the nanoparticles. Increased nanoparticle concentration results in a more pronounced reduction of the velocity and temperature profiles. This phenomenon can be attributed to the rise in the fluid mixture's viscosity due to the volume fraction of the nanoparticles, which acts to limit the rate of momentum transfer to the fluid bulk. While the thermal conductivity of the fluid mixture increases to facilitate the rapid removal of heat, the reduction in the temperature of the bulk fluid will tend to decrease the bulk temperature of the fluid.
- The reduction of the temperature of the bulk fluid will improve the temperature distribution of the fluid, which enhances the thermal characteristics of the fluid. This improved distribution will increase the performance of the fluid in thermal management. The results of this study demonstrate the superiority of hybrid nanofluids relative to base nanofluids. The hybrid nanofluids offer a more effective platform for nanofluid applications due to the presence of multiple nanoparticles, which synergistically enhance the viscous, conductive, and electromagnetic properties.

Nomenclature

Symbol	Description	Symbol	Description
u_s^2	Stretching/ Shrinking velocity $\left(ms^{-1}\right)$	A	Stretching parameter
u and v	x and y components of velocity $\left(ms^{-1}\right)$	x, y	Plane coordinate axis
T_w	Surface temperature	C_{fx}	Coefficient of skin friction

μ_0	Magnetic permeability	a, b, c	Constants
T_∞	Ambient temperature	σ_s	Stefan-Boltzmann constant
ψ	Stream function	q_r	Rosseland for radiation radiative heat flux
T_w	Wall temperature	Nu_x	Nusselt number
k	Thermal conductivity	k_1	Absorption coefficient
Re_x	Reynold number	α	Thermal diffusivity
ρ_{nf}	Nanofluid density	μ	Dynamic viscosity
w	Surface condition	f'	Velocity without dimension
σ	Electrical conductivity of the base fluid	Ec	Eckert number
$\left(\rho c_p\right)_{nf}$	Capacity of heat in nanofluid	ν	Kinematic viscosity
β	Thin film thickness parameter	θ	Temperature without dimension
$B(x)$	Variable magnetic field	Pr	Prandtl number
η	Similarity variable	τ_w	Share stress of wall surface
hnf	Hybrid nanofluid	q_w	Wall heat flux
PDE's	Partial Differential Equations	ODE's	Ordinary Differential Equations

Acknowledgements

The authors gratefully acknowledge the Faculty of Computer Science and Mathematics, Universiti Malaysia Terengganu, for providing partial support for this study. The authors would also like to thank the reviewers for their careful reading of the article and for their helpful remarks.

Conflict of Interest Statement

The authors declare no conflict of interest regarding the publication of this article.

Authors' Contributions

All authors contributed to the conception and design of the study. All authors read and approved the final manuscript. Conceptualisation: Ali Rehman, Zabidin Salleh; Methodology: Ali Rehman, Zabidin Salleh; Formal analysis and investigation: Ali Rehman; Writing - original draft preparation: Ali Rehman; K. Sudarmozhi; Writing - review and editing: Zabidin Salleh; K. Sudarmozhi; Funding acquisition: Zabidin Salleh; Resources: Zabidin Salleh; Validation and visualisation: Ali Rehman, Zabidin Salleh; Supervision: Zabidin Salleh.

References

[1] Suresh, S., Venkitaraj, K. P., Selvakumar, P., & Chandrasekar, M. (2012). Effect of Al2O3Cu/ water hybrid nanofluid in heat transfer. *Experimental Thermal and Fluid Science*, *38*, 54-60.

[2] Ghadikolaei, S. S., Yassari, M., Sadeghi, H., Hosseinzadeh, K., & Ganji, D. D. (2017). Investigation on thermophysical properties of -/ hybrid nanofluid transport dependent on shape factor in MHD stagnation point flow. *Powder Technology*, *322*, 428-438.

[3] Selvakumar, P., & Suresh, S. (2012). Use of --/water hybrid nanofluid in an electronic heat sink. *IEEE Transactions on Components, Packaging and Manufacturing Technology*, *2*(10), 1600-1607. doi**:** 10.1109/TCPMT.2012.2211018

[4] Nasrin, R., & Alim, M. A. (2014). Finite element simulation of forced convection in a flat plate solar collector: Influence of nanofluid with double nanoparticles. *Journal of Applied Fluid Mechanic*, *7*(3), 543-556.

[5] Khan, M., Munawar, S., & Abbasbandy, S. (2010). Steady flow and heat transfer of a Sisko fluid in annular pipe. *International Journal of Heat Mass Transfer*, *53*, 1290-1297.

[6] Khan, M., & Shahzad, A. (2013). On boundary layer flow of a Sisko fluid over a stretching sheet. *Quaestiones Mathematicae*, 36(1), 137–151. https://doi.org/10.2989/16073606.2013.779971

[7] Patel, M., Patel, J., & Timol, M. G. (2015). Laminar boundary layer flow of Sisko fluid. *Applications and Applied Mathematics: An International Journal*, *10*(2), 909-918.

[8] Darji, R. M., & Timol, M. G. (2014). Similarity analysis for unsteady natural convective boundary layer flow of Sisko fluid. *International Journal of Advances in Applied Mathematics and Mechanics*, *1*(3), 22-36.

[9] Siddiqui, A. M., Ashraf, H., Haroon, T., & Walait, A. (2017). On the analytic solution for the steady drainage of magnetohydrodynamic (MHD) Sisko fluid film down a vertical belt. *Applications and Applied Mathematics: An International Journal*, *10*(2), 267-286.

[10] Khan, M., Abbas, Q., & Duru, K. (2010). Magnetohydrodynamic flow of a Sisko fluid in annular pipe: A numerical study. *International Journal for Numerical Methods in Fluids*, *62*, 1169-1180.

[11] G. Sar, M. Pakdemirli, T. Hayat & Y. Aksoy. (2012). Boundary Layer Equations and Lie Group Analysis of a Sisko Fluid. *Journal of Applied Mathematics*, *12*, 1-9. DOI: 10.1155/2012/259608

[12] Khan, I., Khan, M., Malik, M. Y., & Salahuddin, T. (2017). Mixed convection flow of Eyring-Powell nanofluid over a cone and plate with chemical reactive species. *Results in Physics*, *7*, 3716-3722.

[13] Nadeem, S., Ul Haq, R., & Khan, Z. H. (2014). Numerical solution of non-Newtonian nanofluid flow over a stretching sheet. *Applied Nanoscience*, *4*, 625-631.

[14] Rao, J. A., & Buchaiah, C. D. (2019). Finite element solutions of MHD free convective Casson fluid flow towards a vertical plate in presence of hall current, variable suction and heat source. *Pramana Research Journal*, *9*(1).

[15] Rokni, H. B., Alsaad, D. M., & Valipour, P. (2016). Electro hydrodynamic nanofluid flow and heat transfer between two plates. *Journal of Molecular Liquids*, *216(*10), 583-589.

[16] Nadeem, S., Ul Haq, R., & Khan, Z. H. (2014). Numerical solution of non-Newtonian nanofluid flow over a stretching sheet. *Applied Nanoscience*, *4*, 625-631.

[17] Shehzad, S. A., Hayat, T., & Alsaedi, A. (2015). MHD flow of Jeffrey nanofluid with convective boundary conditions. *Journal of Brazilian Society of Mechanical Sciences and Engineering*, *37*(3), 873-883.

[18] Nguyen, C. T., Roy, G., Gauthier, C., & Galanis, N. (2007). Heat transfer enhancement using water nanofluid for an electronic liquid cooling system. *Applied Thermal Engineering*, *27*(8-9), 1501-1506.

[19] Kulkarni, D. P., Vajjha, R. S., Das, D. K., & Oliva, D. (2008). Application of aluminum oxide nanofluids in diesel electric generator as jacket water coolant. *Applied Thermal Engineering*, *28*(14-15), 1774-1781.

[20] Zamzamian, A., Oskouie, S. N., Doosthoseini, A., Joneidi, A., & Pazouki, M. (2011). Experimental investigation of forced convective heat transfer coefficient in the nanofluid / EG and /EG in a double pipe and plate heat exchangers under turbulent flow. *Experimental Thermal and Fluid Science*, *35*(3), 495-502.

[21] Sebdani, S. M., Mahmoodi, M., & Hashemi, S. (2012). Effect of nanofluid variable properties on mixed convection in a square cavity. *International Journal of Thermal Sciences*, *52*, 112-126.

[22] Aaiza, G., Khan, I., & Shafie S. (2015). Energy transfer in mixed convection MHD flow of nanofluid containing different shapes of nanoparticles in a channel filled with saturated porous medium. *Nano scale Research Letters*. https://doi.org/10.1186/s11671-015-1144-4

[23] Ahmed, N., As, A., Khan, U., Mohyud-Din, S. T., & Waheed, A. (2017). Shape effects of nanoparticles on squeezed flow between two Riga plates in the presence of thermal radiation. *The European Physical Journal Plus*, *132*, 321.

[24] Gul, A., Khan, I., Shafie, S., Khalid, A., & Khan, A. (2015). Heat transfer in MHD mixed convection flow of a ferrofluid along a vertical channel. *PLOS One*, *11*(10), 1-14.

[25] Rehman, A., Gul, T., Salleh, Z., Mukhtar, S., Hussain, F., Nisar, K. S., & Kumam, P. (2019). Effect of the Marangoni convection in the unsteady thin film spray of CNT nanofluids. *Processes*, *7*, 392.

[26] Rehman, A., Salleh, Z., Gul, T., & Zaheer, Z. (2019). The impact of viscous dissipation on the thin film unsteady flow of GO-EG/GO-W nanofluids. *Mathematics*, *7*(7), 653.

[27] Liao, S. (2010). An optimal homotopy-analysis approach for strongly nonlinear differential equations. *Communications in Nonlinear Science and Numerical Simulation*, *15(*8), 2003-2016.

[28] Sidahmed, A. O., & Salah, F. (2018). Numerical solution of boundary layer flow of viscous fluid via successive linearization method. *Current Trends in Computer Sciences and Applications*, *1*(2), 28-31.

[29] Ali, A. R., Rafique, K., Imtiaz, M., Jan, R., Alotaibi, H., & Mekawy, I. (2024). Exploring magnetic and thermal effects on MHD bio-viscosity flow at the lower stagnation point of a solid sphere using Keller box technique. *Partial Differential Equations in Applied Mathematics*, *9*, 100601.

[30] Khan, Z., Srivastava, H. M., Mohammed, P. O., Jawad, M., Jan, R., & Nonlaopon, K. (2022). Thermal boundary layer analysis of MHD nanofluids across a thin needle using non-linear thermal radiation. *Mathematical Biosciences and Engineering*, *19*(12), 14116-14141.

[31] Rehman, A., Khan, D., Jan, R., & Mahariq, I. (2024). The impact of Marangoni convection on carbon nanotube blood base hybrid nanofluid with thermal radiation viscous dissipation and couple stress, analytical study. *BioNanoScience*, *14*(2), 814-823.

[32] Rehman, A., Khun, M. C., Salleh, Z., Khan, W., Albely, M. S., Jan, R., & Alhabeeb, S. A. (2023). Analytical study on couple stress flow of GO-EG and GO-W nanofluid over an extending cylinder along with variable viscosity. *Heliyon*, *9*(12).

[33] Zubair, M., Jawad, M., Bonyah, E., & Jan, R. (2021). MHD Analysis of couple stress hybrid nanofluid free stream over a spinning Darcy-Forchheimer porous disc under the effect of thermal radiation. *Journal of Applied Mathematics*, *2021*(1), 2522155.

[34] Rehman, A., Khan, D., Jan, R., Aloqaily, A., & Mlaiki, N. (2023). Scientific exploring of Marangoni convection in stagnation point flow of blood-based carbon nanotubes nanofluid over an unsteady stretching surface. *International Journal of Thermofluids*, *20*, 100470.

[35] Rehman, A., Alhefthi, R. K., Inc, M., & Jan, R. (2024). Analytical investigation of MgO–CuO\ H2O, hybrid nanofluid MHD stagnation point flow with the influence of viscous dissipation for enhancement of heat transfer ratio. *Modern Physics Letters B*, *38*(15), 2450108.

[36] Ahmad, I., Mekawy, I., Khan, M. N., Jan, R., & Boulaaras, S. (2024). Modeling anomalous transport in fractal porous media: A study of fractional diffusion PDEs using numerical method. *Nonlinear Engineering*, *13*(1), 20220366.

[37] Rehman, A., Khan, W., Abdelrahman, A., Jan, R., Khan, M. S., & Galal, A. M. (2022). Influence of Marangoni convection, solar radiation, and viscous dissipation on the bioconvection couple stress flow of the hybrid nanofluid over a shrinking surface. *Frontiers in Materials*, *9*, 964543.

[38] Rehman, A., Saeed, A., Salleh, Z., Jan, R., & Kumam, P. (2022). Analytical investigation of the time-dependent stagnation point flow of a CNT nanofluid over a stretching surface. *Nanomaterials*, *12*(7), 1108.

[39] Rehman, A., Khun, M. C., Rezapour, S., Inc, M., Garalleh, H. A., & Muhammad, T. (2024). Analytical analysis and heat transfer of CuO and MgO engine oil base nanofluid with the influence of dynamic viscosity, magnetic field, and convective boundary conditions. *ZAMM-Journal of Applied Mathematics and Mechanics/Zeitschrift für Angewandte Mathematik und Mechanik*, *104*(6), e202300510.

[40] Khan, A., ul Karim, F., Khan, I., Ali, F., & Khan, D. (2018). Irreversibility analysis in unsteady flow over a vertical plate with arbitrary wall shear stress and ramped wall temperature. *Results in Physics*, *8*, 1283-1290.

[41] Khan, D., Kumam, P., Khan, I., Sitthithakerngkiet, K., Khan, A., & Ali, G. (2022). Unsteady rotating MHD flow of a second-grade hybrid nanofluid in a porous medium: Laplace and Sumudu transforms. *Heat Transfer*, *51*(8), 8065-8083.

[42] Rehman, A., Khan, D., Jan, R., Aloqaily, A., & Mlaiki, N. (2023). Scientific exploring of Marangoni convection in stagnation point flow of blood-based carbon nanotubes nanofluid over an unsteady stretching surface. *International Journal of Thermofluids*, *20*, 100470.

[43] Khan, D., Kumam, P., & Watthayu, W. (2021). A novel comparative case study of entropy generation for natural convection flow of proportional-Caputo hybrid and Atangana baleanu fractional derivative. *Scientific Reports*, *11*(1), 22761.

[44] Khan, A., ul Karim, F., Khan, I., Alkanhal, T. A., Ali, F., Khan, D., & Nisar, K. S. (2019). Entropy generation in MHD conjugate flow with wall shear stress over an infinite plate: Exact analysis. *Entropy*, *21*(4), 359.

[45] Sooppy Nisar, K., Khan, D., Khan, A., Khan, W. A., Khan, I., & Aldawsari, A. M. (2019). Entropy generation and heat transfer in drilling nanoliquids with clay nanoparticles. *Entropy*, *21*(12), 1226.